IJIRSET
International Journal of Innovative Research in Science | Engineering | Technology

ISSN(O): 2319-8753
ISSN(P): 2347-6710

International Journal of Innovative Research in Science Engineering and Technology (IJIRSET)

(A Monthly, Peer Reviewed, Refereed, Scholarly Indexed, Open Access Journal)

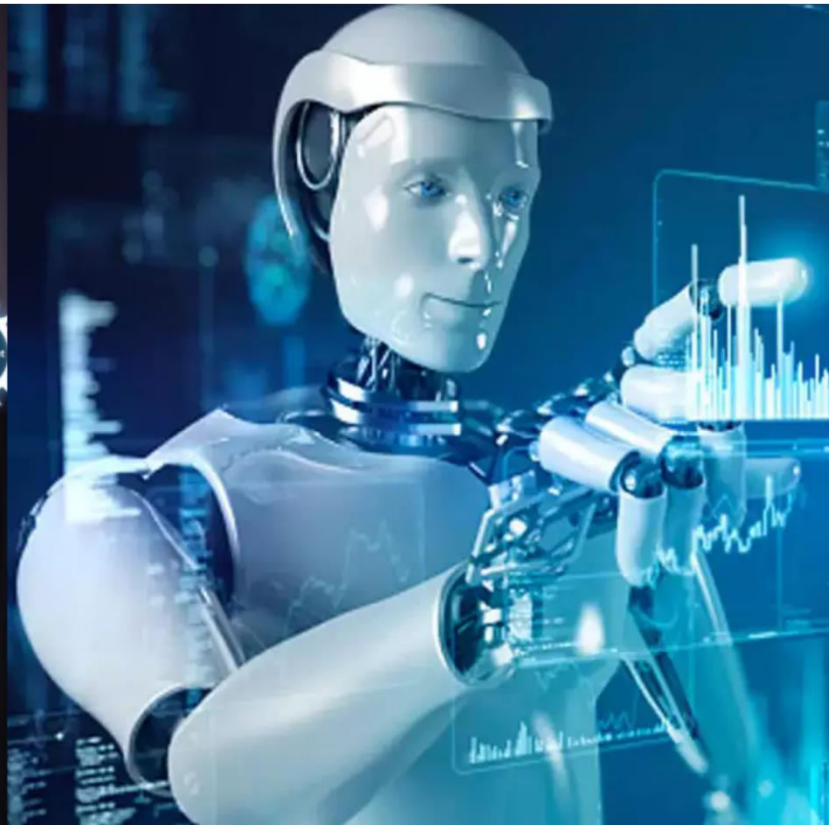

Impact Factor: 8.699

Volume 14, Issue 12, December 2025

International Journal of Innovative Research of Science, Engineering and Technology (IJIRSET)

Impact Factor 8.699

|www.ijirset.com |A Monthly, Peer Reviewed & Refereed Journal| e-ISSN: 2319-8753| p-ISSN: 2347-6710|

Volume 14, Issue 12, December 2025

|DOI: 10.15680/IJIRSET.2025.1412008|

Research on Structural Spatial Damage Identification Based on 3D-Slicing Method

Renling Huang[a], Jia Guo[b], Junping Zhong[c], Zhuo Li[a]

College Student, College of Civil Engineering, Hunan City University, Yiyang, Hunan, China[a]

Lecturer, College of Civil Engineering, Hunan City University, Yiyang, Hunan, China[b]

Teaching Assistant, College of Civil Engineering, Hunan City University, Yiyang, Hunan, China[c]

ABSTRACT: A damage identification method based on Three-Dimensional-Slicing(3D-Slicing) method is proposed for the spatial damage identification of structures. The beam structural spatial damage is taken as the research object and the strain mode is taken as the damage identification parameter. The 3D-Slicing method is used to slice the beam structural three-dimensional space to the obtain strain modes of different dimensions, which are transformed by continuous wavelet to obtain the corresponding wavelet coefficients, and then the coordinates of damage locations in each dimension are identified based on the singularity of the wavelet coefficient values, thereby the beam structural spatial damage are located. After the damage location is identified, the improved particle swarm optimization algorithm (IPSO), proposed in this study, is used to identify the severity and size of the damage location.The numerical simulation and experiment results of the fixed beam structure show that the structural spatial damage identification method based on 3D-Slicing can effectively identify the beam structural spatial damage, and can also effectively solve the problem that the edge effect of the wavelet coefficient makes the edge damage to be difficult to identify. The proposed method opens up a new approach for identifying the location of structural spatial damage, and provides a theoretical basis and technical mean for identifying spatial damage in actual structures.

KEYWORDS: 3D-Slicing; Wavelet coefficients; IPSO; Beam structure experiment; Spatial damage identification

I. INTRODUCTION

With the popularization of large-scale structures, the structural forms are becoming more and more complex. The damaged structure during service may eventually lead to structural failure as the damage progresses, and result in significant safety accidents. Therefore, it is particularly important to conduct health monitoring on structures, and structural damage diagnosis is the most basic and important part of health monitoring, which provides the most basic data support for structural health monitoring. At present, the structural damage identification methods based on wavelet transform and intelligent algorithm still remain one-dimensional and two-dimensional [1,2], but the accuracy of one-dimensional and two-dimensional damage identification has gradually failed to meet the requirements of structural health monitoring, and a more perfect method is needed to identify structural spatial damage.

The structural damage identification method based on vibration response is a commonly used approach for identifying structural damage, which does not need to damage the structure. Experts and scholars, in related fields, have used the structural vibration response for detecting damage in recent decades [3-6], and relevant methods are proposed[7,8]. For example, the damage identification method of calculating modal strain energy by modal shape is adopted, and the effectiveness of this method for damage location of complex structures is verified through numerical simulation [9]; There is also a wavelet transform method based on curvature mode to identify the damage of beams on elastic foundation, and numerical simulation has proved that this method can effectively identify the damage location [10]. Previous studies have shown that the strain mode is more sensitive to damage than displacement mode and curvature mode [11], and the structural damage identification method based on strain mode is to identify the damage by establishing damage index and obtaining the change of damage index before and after structural damage. The numerical simulation and experiment results of relevant studies show that the structural damage identification method based on strain mode can accurately identify the structural damage location, and has better noise resistance than the modal strain energy damage identification method based on displacement mode [12,13]. The modal shape of the damaged structure are unsmooth and discontinuous [14], so the structural damage identification can be diagnosed

International Journal of Innovative Research of Science, Engineering and Technology (IJIRSET)

Impact Factor 8.699

|www.ijirset.com |A Monthly, Peer Reviewed & Refereed Journal| e-ISSN: 2319-8753| p-ISSN: 2347-6710|

Volume 14, Issue 12, December 2025

|DOI: 10.15680/IJIRSET.2025.1412008|

without prior knowledge of the undamaged structure based on this concept. Therefore, the detection of modal shape discontinuity in the structural damage area is the main indicator of damage detection based on vibration in this study.

Wavelet transform is widely used in the field of structural health monitoring because of its excellent denoising ability and singularity detection characteristics. The singularity of the structural mode shape can be quickly found by wavelet transform,which can intuitively display the structural damage location [15], therefore, the method of detecting structural modal shape discontinuity based on wavelet singularity has attracted researchers' attention. Zhu and Law [16] excite the bridge structure to obtain the displacement modes by the moving load, and then the bridge structural displacement modes are analyzed through continuous wavelet transform (CWT) to identify the crack location along the length direction of the bridge. He et al. [17] proposed to use moving loads to excite the bridge to obtain the displacement response, which is decompose by discrete wavelet transform (DWT) to locate the potential damage location of the structure. Zhou and Chen [18] proposed a damage identification method based on curvature mode and two-dimensional continuous wavelet transform to identify the planar damage location of composite sandwich panels, which deal with the curvature mode by two-dimensional continuous wavelet transform and combine structural periodicity and wavelet transform coefficients to construct the damage indicator. Finally, the structural damage is identified.

Particle swarm optimization algorithm (PSO) is widely used in many disciplines because of its powerful optimization ability, simple use, fast convergence and good robustness [19].When identifying structural damage, PSO describes the damage problem as an objective function problem, that is solved to identify the structural damage [20].However, PSO is prone to fall into prematurity and local optimal solutions, resulting in low computational efficiency and accuracy. According to the shortcomings of PSO, relevant experts have proposed corresponding improvement methods for the problems to be solved [21,22].Minh H L et al. [23] proposed a variable velocity strategy particle swarm optimization algorithm (VVS-PSO) to solve the problems of structural optimization and damage assessment. VVS-PSO introduced a new term in the speed update process of each iteration, which was controlled by a reduced linear function, so that VVS-PSO could achieve faster convergence speed and higher accuracy, which was proved to be effective by the experiment of a four-layer steel frame. Khatir proposed a two-stage damage identification method based on normalized modal strain energy. This method is based on the principle that structural damage causes changes in modal parameters, and combined with artificial neural network (ANN), PSO and nMSEDI to train and update the damage model, to achieve the purpose of accurately identifying the beam structural damage severity.

At present, the structural damage identification method based on wavelet transform and PSO still remains at the one-dimensional and two-dimensional levels, that is, the length direction of the beam structure and the plane damage of the plate structure, the spatial damage identification problem of the structure has not been solved by the relevant knowledge and method of wavelet transform and PSO. Moreover, due to the edge effect of the wavelet coefficients, it is difficult to identify the structural edge damage directly through the singularity of the wavelet coefficients [25].

In summary, this study proposes a spatial damage identification method based on 3D-Slicing. Firstly, the beam structural dimension is reduced by 3D-Slicing method, which separating the strain modal data of different dimensions. Then, the strain modal data of different dimensions are transformed by wavelet to obtain the wavelet coefficients, and the singularities of the data of different dimensions are identified according to the singularity principle of the wavelet coefficients. Based on the relationship between the singular point values of wavelet coefficients of different data in the same dimension, the beam structural spatial damage location is identified. A new improved particle swarm optimization (IPSO) algorithm is proposed to improve the learning factor calculation method of PSO, which makes the IPSO hardly fall into the precocity and local optimal solution, and then the IPSO is used to identify the damage severity and size of the beam structure. The effectiveness of the proposed method is verified by numerical simulation and experimental analysis of the fixed beam structure.

II. THEORETICAL BACKGROUND

2.1. 3D-Slicing method

In this study, based on the beam structural multi-dimensional characteristics, the beam structure is meshed in the direction of length, width and height respectively according to the requirements, as shown in Figure 1. Three-dimensional slices, after the beam structural grid division, are made on the gridlines in the long, wide and high directions along the beam length direction to achieve dimensionality reduction, to make the spatial damage coordinates

International Journal of Innovative Research of Science, Engineering and Technology (IJIRSET)

Impact Factor 8.699

|www.ijirset.com |A Monthly, Peer Reviewed & Refereed Journal| e-ISSN: 2319-8753| p-ISSN: 2347-6710|

Volume 14, Issue 12, December 2025

|DOI: 10.15680/IJIRSET.2025.1412008|

unidimensional. According to the analysis of each one-dimensional path in the three-dimensional section of the beam structure, the damage parameter data in each dimension direction is obtained. Then, the corresponding wavelet coefficient graph is obtained by the wavelet transform of each dimensional data, and the damage location coordinates h_i , b_i , l_i of each dimension are identified based on the singularity of the wavelet coefficient graph. Finally, the overall three-dimensional damage coordinates (h_i , b_i , l_i) of the beam structure can be obtained by synthesizing the damage location coordinates of each dimension, to achieve the purpose of identifying the beam structural spatial damage.

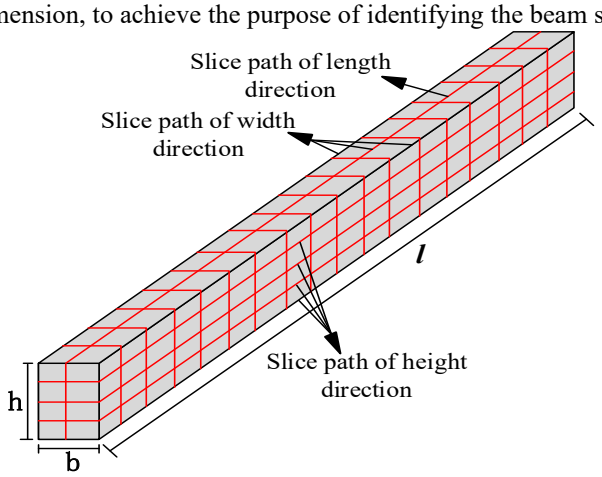

Figure 1: Grid division of the beam

2.2.The Principle of Wavelet Singularity

Considering the function, $\psi(t) \in L^1(R) \cap L^2(R)$, and $\int_{-\infty}^{+\infty} \psi(t)dt = 0$, $\psi(t)$ is called a basic wavelet or a mother wavelet. $\psi(t)$ is scaled and translate as:

$$\psi_{a,b}(t) = \frac{1}{\sqrt{|a|}} \psi\left(\frac{t-b}{a}\right), a, b \in R, a \neq 0 \quad (1)$$

where a and b are the scale factor and translation factor respectively, and $\psi_{a,b}(t)$ is wavelet function.

Defining $\psi(t)$ as the basic wavelet, the continuous wavelet transform(CWT) of $f(t) \in L^2(R)$ is defined as:

$$Wf(a,b) = \frac{1}{\sqrt{|a|}} \int_{-\infty}^{+\infty} f(t)\psi^*\left(\frac{t-b}{a}\right)dt = \langle f, \psi_{a,b} \rangle \quad (2)$$

where $a \neq 0, b, t$ is continuous variable and $\psi^*(t)$ is the complex conjugate of $\psi(t)$.

The convolution form of wavelet transform is:

$$Wf(a,b) = \frac{1}{\sqrt{|a|}} \int_{-\infty}^{+\infty} f(t)\psi^*\left(\frac{t-b}{a}\right)dt = \sqrt{|a|} f * \hat{\psi}_{|a|}(b) \quad (3)$$

where $\hat{\psi}_{|a|}(t) = |a|^{-1} \psi^*(-t/a)$.

Defining $\theta(t)$ as a smooth function and derivative, $\psi(t) = \frac{d\theta(t)}{dt}$, of any low-pass function $\theta(t)$ is band-pass function, which satisfies $\int_{-\infty}^{+\infty} \psi(t)dt = 0$, and the wavelet function with scale factor s is:

International Journal of Innovative Research of Science, Engineering and Technology (IJIRSET)

Impact Factor 8.699

|www.ijirset.com |A Monthly, Peer Reviewed & Refereed Journal| e-ISSN: 2319-8753| p-ISSN: 2347-6710|

Volume 14, Issue 12, December 2025

|DOI: 10.15680/IJIRSET.2025.1412008|

$$\psi_s(t)=\frac{1}{s}\psi\left(\frac{t}{s}\right)=\frac{1}{s}\frac{d\theta\left(\frac{t}{s}\right)}{dt}=\frac{d\theta_s(t)}{dt} \tag{4}$$

The continuous wavelet transform of the basic wavelet corresponding to function f on s is:

$$Wf(s,u)=s^{1/2}\left(f*\bar{\psi}_s\right)(u)=s^{1/2}\frac{d}{du}\left(f*\bar{\theta}_s\right)(u) \tag{5}$$

where $s>0$, and equation 5 shows that the modulus maximum $|Wf(s,u)|$ of the wavelet transform is the maximum of the first derivative of f smoothed by $\bar{\theta}_s$, and corresponds to the singular point of signal.

2.3 IPSO

PSO：The particle swarm is defined to find the optimal solution in a *M*-dimensional solution space, and the swarm initialized with N random particles, the position X_i of the i particle is $X_i=(x_{i1},x_{i2},\cdots,x_{iM})$, and the velocity V_i is $V_i=(v_{i1},v_{i2},\cdots v_{iM}),i=1,2,\cdots,N$,and x and v are the components of X and V in different dimensions, respectively. In the iterative optimization process, the particles will evaluate the current position by the established fitness function $f(x)$, and the individual optimal position $p_{best}=(p_{i1},p_{i12},\cdots p_{iM})$ of each particle in the current group and the global extreme value of the whole group are evaluated according to equations (6) and (7).

$$p_{best}(k+1)=\begin{cases}p_{best_i}(k) & f\left[X_i(k+1)\right]\geq f\left[p_{best_i}(k)\right]\\ X_i(k+1) & f\left[X_i(k+1)\right]<f\left[p_{best_i}(k)\right]\end{cases} \tag{6}$$

$$g_{best}(k)=\min\left\{f\left[p_{best_1}(k)\right],f\left[p_{best_2}(k)\right],\cdots,f\left[p_{best_N}(k)\right]\right\} \tag{7}$$

$$v_{im}^{k+1}=wv_{im}^{k}+c_1r_1\left(p_{im}^{k}-x_{im}^{k}\right)+c_2r_2\left(g_{im}^{k}-x_{im}^{k}\right) \tag{8}$$

$$x_{im}^{k+1}=x_{im}^{k}+v_{im}^{k} \tag{9}$$

where k is the number of current iteration steps; $i=1,2,\cdots,N$, $m=1,2,\cdots,M$; w is the inertia weight factor, which is calculated by equation 10, and $w_{\max}=0.9$, $w_{\min}=0.4$. r_1,r_2 are the random values in [0,1]. c_1 and c_2 control the self-learning ability and social learning ability of particles respectively. In the early stage of PSO operation, it is required to strengthen the global search ability, so the particle needs to strengthen the self-learning ability and weaken the social learning ability; In the late stage of particle swarm optimization, it is necessary to strengthen the social learning ability and weaken the self-learning ability to converge the results to the global optimal solution. Therefore, the inverse change calculation method is adopted for c_1 and c_2, and the calculation formulas are shown in equations (11) and (12), respectively.

$$w=w_{\max}-\frac{t\times\left(w_{\max}-w_{\min}\right)}{T} \tag{10}$$

$$c_1=c_1^i+\frac{c_1^f-c_1^i}{T}\times t \tag{11}$$

$$c_2=c_2^f+\frac{c_2^i-c_2^f}{T}\times t \tag{12}$$

Where, c_1^i , c_2^i are the initial values of c_1 and c_2 respectively, c_1^f , c_2^f are the final values of c_1 and c_2 respectively. This study takes $c_1^i=c_2^i=2$， $c_1^f=c_2^f=0.5$.

The steps required for IPSO to identify the structural damage severity are as follows:

International Journal of Innovative Research of Science, Engineering and Technology (IJIRSET)

Impact Factor 8.699

|www.ijirset.com |A Monthly, Peer Reviewed & Refereed Journal| e-ISSN: 2319-8753| p-ISSN: 2347-6710|

Volume 14, Issue 12, December 2025

|DOI: 10.15680/IJIRSET.2025.1412008|

1. Establishing the unknown function: The damage severity of the structural damage element is simulated by element stiffness reduction, and the relationship between the stiffness of the damaged element and its undamaged stiffness is as follow:

$$EI_i = \gamma_i EI \tag{13}$$

Where, E is the elastic modulus, and it is assumed that E remains unchanged. I and $I^{'}$ are the moment of inertia of the undamaged element and the moment of inertia of the damaged element, respectively. γ_i is the damage severity of element *i*.

2. Constructing the objective function: The weighted sum method of frequency change function and displacement mode change function are combined to construct the objective function, as shown in equation (14).

$$\min F = F_\omega \sum_{i=1}^{m} \left(\frac{f_i^{test} - f_i^{cal}(\gamma)}{f_i^{test}} \right)^2 + F_\phi \sum_{i=1}^{n} \sum_{j=1}^{k} \left(\phi_{ij}^{test} - \phi_{ij}^{cal}(\gamma) \right)^2 \tag{14}$$

where F_ω and F_ϕ are weighting factors, which are set as 1; f_i^{test} and f_i^{cal} are the i-th order natural frequencies measured and calculated respectively; ϕ_{ij}^{test} and ϕ_{ij}^{cal} are the displacement modes of the i-th order j-th node measured and calculated respectively after normalization; m is the order of natural frequency, n is the order of displacement mode, and k is the node number. The unknown value γ of the minimum value of the objective function $\min F$ is the set of damage severity γ_i of all damaged elements of the structure.

3. Establishing fitness function: $\min F$ is taken as the fitness function $FIT1$ of IPSO to identify the structural damage severity, i.e. $FIT1 = \min F$. The particles of the group search for the optimal solution in the solution space based on the minimum value of $\min F$.

4. Setting IPSO parameters: The number of structural damage elements is the dimension *M* of particles; The value of particle n ranges from 0 to 0.9, and the number of particles N ranges from 50 to 100; w is calculated with equation (10), the values of c_1 and c_2 are calculated with equations (11) and (12), respectively; The maximum value of iterations T is set to 100; The accuracy error e of the optimal solution is set to 0.0001.

After the relevant parameters are set, it is necessary to adjust the parameters of the established model based on experimental data to eliminate modeling errors as much as possible. Then the IPSO code is debugged according to the required optimization problem, and the parameter settings are determined, to complete the identification of the structural damage severity.

In this study, the termination conditions of IPSO are set as follows: (1) The maximum number of iterations *T*=100; (2) The calculated optimal solution satisfies the requirement of precision. Either of these two conditions is satisfied, IPSO terminates the iteration and outputs the current optimal solution.

Figure 2 shows the flowchart of the method proposed in this study for identifying structural damage:

International Journal of Innovative Research of Science, Engineering and Technology (IJIRSET)

Impact Factor 8.699

|www.ijirset.com |A Monthly, Peer Reviewed & Refereed Journal| e-ISSN: 2319-8753| p-ISSN: 2347-6710|

Volume 14, Issue 12, December 2025

|DOI: 10.15680/IJIRSET.2025.1412008|

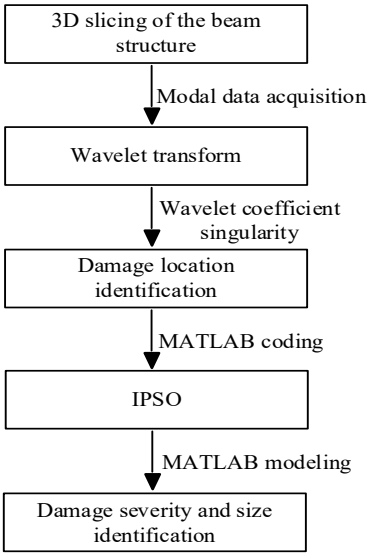

Figure 2: Damage identification flow chart

2.4 Strain Modal Calculation Method

Strain is the first derivative of the displacement, so each displacement mode corresponds to the corresponding strain mode, and the strain mode reflects the inherent characteristics of the structure. To measure the strain, the curvature mode can be used for indirect measurement. According to the material mechanics, the bending static relation of the beam can be obtained as:

$$\rho_i = \frac{1}{d_i} = \frac{M_i}{E_i I_i} \tag{15}$$

Where, i is the section position of measuring point i, M_i is the bending moment of the section i, $E_i I_i$ is the flexural rigidity of the section i, d_i is the radius of curvature at the section i, and ρ_i is the curvature of the section i. According to the approximate equation of bending deformation of the beam:

$$\rho = \frac{d^2 y}{dx^2} \tag{16}$$

where, x is the coordinate along the length direction of the straight beam, and y is the bending deflection of the beam. According to equations (15) and (16), the difference equation of three equidistant continuous measuring points along the beam can be obtained:

$$\rho_i = \frac{M_i}{E_i I_i} = \frac{y_{i+1} - 2y_i + y_{i-1}}{\Delta^2} \tag{17}$$

where i-1, i and i+1 are three adjacent continuous measuring points with equal distance along the beam, ρ_i is the curvature of the section i, y_i is the bending deflection of the section i, y_{i+1} and y_{i-1} are the bending deflection of the section i-1 and the section i+1 of the measuring points respectively, and Δ is the bending deflection of two adjacent measuring points. The strain ε_i of the measuring point i of the beam can be expressed as:

$$\varepsilon_i = -\frac{h}{d_i} = -h\frac{y_{i+1} - 2y_i + y_{i-1}}{\Delta^2} = -h\rho_i \tag{18}$$

where h is the distance between the surface of the measuring point on the beam and the neutral layer, and equation (18) shows the direct relationship between the curvature mode and the strain mode of the beam.

2.5. Mother wavelet Selection

International Journal of Innovative Research of Science, Engineering and Technology (IJIRSET)

Impact Factor 8.699

|www.ijirset.com |A Monthly, Peer Reviewed & Refereed Journal| e-ISSN: 2319-8753| p-ISSN: 2347-6710|

Volume 14, Issue 12, December 2025

|DOI: 10.15680/IJIRSET.2025.1412008|

To obtain the mother wavelet of the wavelet transform required in this study, a fixed-supported rectangular beam is selected as the research object. The beam length $L=1274mm$, section size $b\times h=60mm\times 80mm$ and parameters of the beam are shown in Table 1. The beam fixed at both ends is evenly divided into 49 elements along the length direction, and the element nodes are numbered successively from No. 1 at the left end to No. 50 at the right end. The damage scenarios are shown in Table 2. The damage severity of the beam is simulated by the stiffness reduction method, and the data of the central axis on the surface of the beam as shown in Figure 1 is taken as the calculation data.

ANSYS software is used to model the beam to obtain the first-order curvature mode, and MATLAB is used to calculate the corresponding strain mode through first-order difference. The first-order difference results in one less number of strain modal data corresponding to the original data. Haar wavelet, Db wavelet, Mexh wavelet, Morle wavelet and Meyer wavelet are selected to transform the modal data respectively, and the most suitable mother wavelet is obtained by comparing the wavelet coefficient graphs of these five wavelet functions. Figure 3 shows the wavelet coefficients of the first-order strain mode transformation of the beam structure by five kinds of wavelets.

Table 1: Parameters of the beam

Parameter	Value
ρ	$7800kg/m^3$
μ	0.3
E	$2.1\times10^{11}N/m^3$

Table 2: Damaged scenarios

Number	1
location	Element 25 on the bottom of the beam
Form	Uniform damage of equal height penetration
Severity	10%

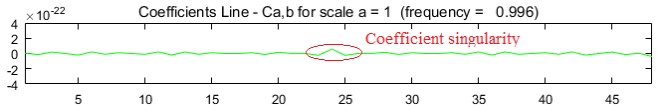

(a)

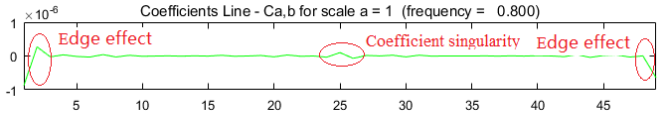

(b)

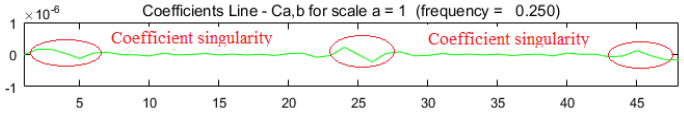

(c)

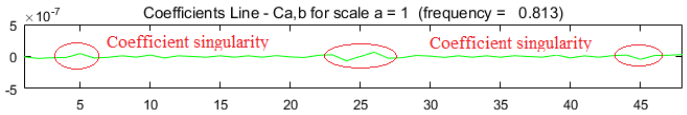

(d)

International Journal of Innovative Research of Science, Engineering and Technology (IJIRSET)

Impact Factor 8.699

|www.ijirset.com |A Monthly, Peer Reviewed & Refereed Journal| e-ISSN: 2319-8753| p-ISSN: 2347-6710|

Volume 14, Issue 12, December 2025

|DOI: 10.15680/IJIRSET.2025.1412008|

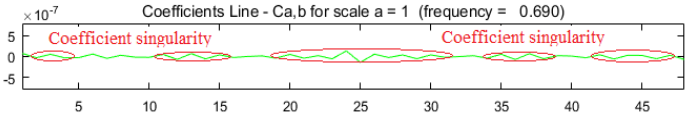

(e)

Figure 3: Wavelet transform coefficients of 5 kinds of wavelets. (a) Haar wavelet transform coefficient. (b) Db3 wavelet transform coefficient. (c) Mexh wavelet transform coefficient. (d)Morle wavelet transform coefficient. (e)Meyer wavelet transform coefficient.

From Figure 3, it can be seen that the wavelet coefficient graph corresponding to Haar wavelet and Db3 wavelet exhibit singularities at the damage location of element 25, while the wavelet coefficient graph corresponding to Mexh wavelet, Morle wavelet, Meyer wavelet exhibit errors in identifying damage, even failing to identify damage. Therefore, Haar wavelet and Db3 wavelet can better identify the structural damage location based on vibration signals in theory. However, the damage location can be identified is not enough in theory, and it is also necessary to observe the performance of the mother wavelet in actual structural damage identification. As Mexh wavelet, Morle wavelet and Meyer wavelet are verified not to be the mother wavelet function of structural damage identification in theory, only Haar wavelet and Db3 wavelet need to be verified through damage identification experiments.

A rectangular Q235 steel beam, with the length $L=1300mm$, was taken as the experiment object. The parameters of the beam were shown in Table 1. The beam was evenly divided into 49 elements along the length direction, and 13mm was left at each end of the beam as the installation position for sensors. A force hammer was used to excite the beam, and 16 high-sensitivity vibration sensors were used to obtain the first-order displacement modal data. The strain mode is obtained by second-order difference of the displacement mode through MATLAB, and then the strain mode is transformed by wavelet to obtain the wavelet coefficient graph of Haar wavelet and Db3 wavelet as shown in Figure 4. The second-order difference will reduce the number of the strain data corresponding to the original mode data in the wavelet coefficient graph by two. It can be seen from Figure 4 (a) that the edge effect at both ends of the Haar wavelet transform coefficient graph are asymmetric and irregular, and a misjudgment occurred at point 42, and the edge effect rule in Figure 3 (a) is not as obvious as the edge effects in Figure 4 (a). The edge effect characteristics of the Db3 wavelet transform coefficient graph in Figure 4 (b) are the same as those in Figure 3 (b), and the wavelet coefficient graph of the Db3 wavelet transform in Figure 4 (b) shows the singularity at the damaged position, while there is no singularity at the undamaged position, and the wavelet transform coefficient of Db3 does not show damage misjudgment.

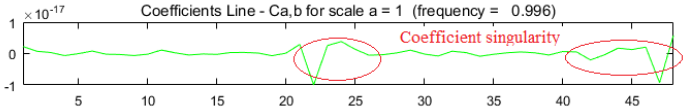

（a）

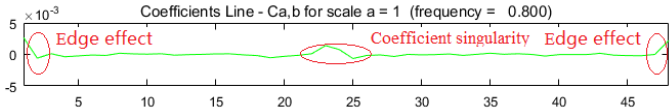

（b）

Figure 4: Two types of wavelet transform coefficient graph in the experiment. （a）Haar wavelet transform coefficient graph. （b）Db3 wavelet transform coefficient graph

Numerical simulation and experimental analysis have shown that Db3 wavelet is the most suitable mother wavelet for structural damage identification in this study through trial-and-error method, and the compact support, vanishing moment and regularity of Db3 are the best match with the structural damage identification based on vibration, which can bring the best resolution and recognition effect to the wavelet coefficient graph of structural damage identification. Moreover, the resolution of the wavelet coefficient graph provided by the first-order strain mode of the beam structure is good. Therefore, Db3 wavelet and the first-order strain mode of the beam structure are selected for structural damage identification in this study.

International Journal of Innovative Research of Science, Engineering and Technology (IJIRSET)

Impact Factor 8.699

|www.ijirset.com |A Monthly, Peer Reviewed & Refereed Journal| e-ISSN: 2319-8753| p-ISSN: 2347-6710|

Volume 14, Issue 12, December 2025

|DOI: 10.15680/IJIRSET.2025.1412008|

III. NUMERICAL SIMULATION

To verify the effectiveness of the 3D-slicing method in the spatial damage identification of the beam structure, a fixed beam was used as the model for numerical simulation analysis, as shown in Figure. 5. The damage identification method based on wavelet transform has been proved to have strong robustness [29-30], so a repeated verification of anti-noise performance is not carried out in this study.

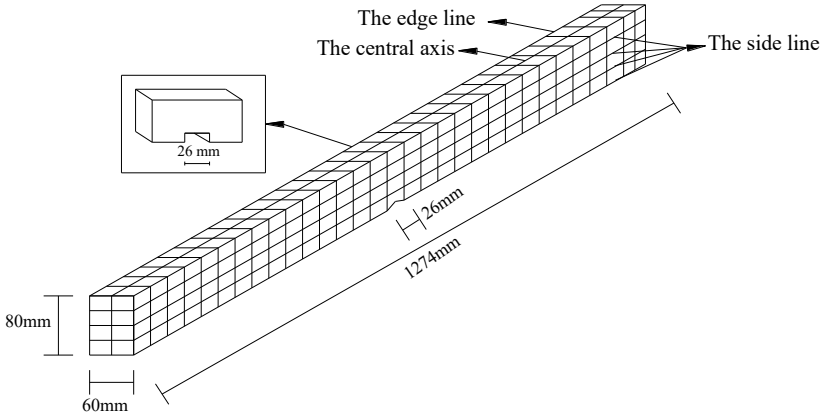

Figure 5: The fixed beam model

The beam structural modeling parameters: The length $L=1274mm$, section size $b\times h=60mm\times 80mm$ and parameters are shown in Table 1. The two ends of the beam are fixed. The beam is evenly divided into 49 elements along the length direction, which are numbered from left to right. The beam is evenly divided into 2 elements along the width direction and divided into 4 elements along the side height direction (that is, divided into 4 layers along the side height direction of the beam). The grid composed of the element nodes is the three-dimensional measurement point grid of the beam structure. The data of the element nodes are taken as the data required for numerical simulation, and the data B_1^N of the first column near the side of the upper surface along the length direction is the data of the first layer on the side, and then the data of the second B_2^N, third B_3^N, fourth B_4^N layers on the side are successively approached to the lower surface of the beam. The central axis of the upper surface of the beam along the length direction is taken as a set of damage data.

The damage scenario of the beam is shown in Table 3. On the lower surface of the beam structure, elements 12, 25 and 49 along the length direction are set equal height uniform damage along the beam thickness direction. The damage coordinates in the beam width direction can be located without identification, and the spatial damage location can be identified only by locating the coordinates in the beam length and height direction. Since the data length along the beam height direction is short, the strain modal data along the length direction at different heights on the side of the beam can be measured, and the damage coordinates can be determined by comparing the wavelet coefficient singularity of the data of different heights. Therefore, a total of 5 sets of data for numerical simulation are needed to take, which including the axis data along the length direction on the upper surface of the beam and 4 layers of data along the length direction at different heights on the side. To facilitate the comparison of wavelet coefficients in the same dimension, each set of strain modal data is normalized. The normalization formula is shown in equation (19).

$$C_i(t)=\frac{K_i(t)}{K_i(MAX)} \tag{19}$$

Where, $K_i(t)$ represents the *t*-th data of group *i*, $K_i(MAX)$ represents the maximum value in group *i*, and $C_i(t)$ represents the *t* th data of group *i* normalized data.

The ANSYS software is used for the beam structural modeling. The first-order curvature modal data of the beam can be directly obtained through software analysis, and then the corresponding strain modal data can be obtained through first-order differential calculation.

International Journal of Innovative Research of Science, Engineering and Technology (IJIRSET)

Impact Factor 8.699

|www.ijirset.com |A Monthly, Peer Reviewed & Refereed Journal| e-ISSN: 2319-8753| p-ISSN: 2347-6710|

Volume 14, Issue 12, December 2025

|DOI: 10.15680/IJIRSET.2025.1412008|

Table 3: Damage scenario of the beam

Element number	Element size （mm）	Damage location coordinates (h_i , b_i , l_i)	Damage form	Damage severity γ	Damage depth a（mm）
49	26	(4, 0, 12)	Uniform damage through equal height	5%	1.36
		(4, 0, 25)		20%	5.34
		(4, 0, 49)		10%	2.76

3.1 Identification of Damage location

The strain modal data was transformed by wavelet to obtain the wavelet coefficient diagram as shown in Figure 6. Figure 6 (a) shows that the singularity point of the wavelet coefficient obtained by the wavelet transform on the strain mode of the central axis of the beam structural upper surface is at node 25, which corresponds to element 25. Therefore, element 25 along the length direction of the beam structure is the damage element, but it is impossible to determine the damage location in the beam height direction. Due to the influence of edge effect, it is difficult to determine whether there is damage in element 49, and the micro singularity of the wavelet coefficient of element 12 makes it difficult to determine whether there is damage. It can be seen from Figure 6 (b) ~ (c) that the strain mode wavelet coefficients of the first and second layers on the side of the beam are smooth without obvious singularity except for the end points, which indicates that the first and second layers on the side of the beam have no damage along the length direction. Figure 6 (d) ~ (e) also show that as the wavelet coefficient graph gets closer and closer to the damage position layer, that is, the fourth layer on the side of the beam, the wavelet coefficient of element 25 corresponding to node 25 gradually shows singularity and increases gradually. The wavelet coefficient singularity of element 25 in Figure 6 (e) is the largest. After a comprehensive comparison of the wavelet coefficient singularity values in Figure 6 (b) ~ (e), it is indicated that the damage of element 25 is located at the fourth layer. It can also be seen from Figure 6 (b) ~ (e) that as the wavelet coefficient graphs get closer and closer to the damage layer, the singularity range of the wavelet coefficient and the value of the wavelet coefficient at the right edge of the beam also gradually increase, while the singularity range of the wavelet coefficient and the value of the wavelet coefficient at the left end of the beam do not change, which indicating that there is damage at the fourth layer at the right end of the beam, but the specific location of the damage cannot be determined. The above analysis shows that the beam structural damage is located at element 25 and the rightmost element on the bottom of the beam, and it is concluded that the absolute value of the corresponding wavelet coefficient singular and the range of the wavelet coefficient singularity will increase with the increase of the damage severity under the same scenario. The proposed method is proved to be effective in identifying the spatial damage location of the beam structure, but it is difficult to identify the micro-damage less than 5%.

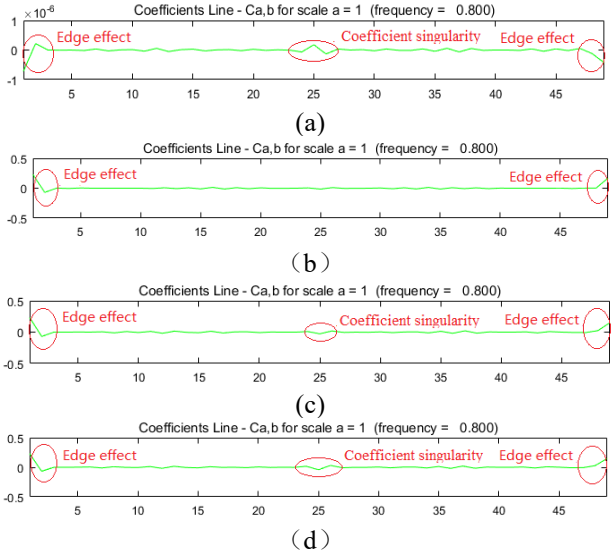

International Journal of Innovative Research of Science, Engineering and Technology (IJIRSET)

Impact Factor 8.699

|www.ijirset.com |A Monthly, Peer Reviewed & Refereed Journal| e-ISSN: 2319-8753| p-ISSN: 2347-6710|

Volume 14, Issue 12, December 2025

|DOI: 10.15680/IJIRSET.2025.1412008|

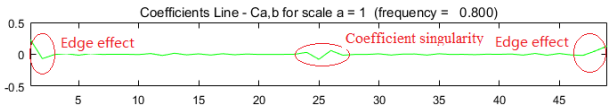

(e)

Figure 6: Wavelet coefficients of strain modes of the beam structural upper surface and lateral surface. (a) The strain mode wavelet coefficients of the central axis of the beam structural upper surface. (b) The strain mode wavelet coefficient diagram of B_1^N . (c) The strain mode wavelet coefficient diagram of B_2^N . (d) The strain mode wavelet coefficient diagram of B_3^N . (e) The strain mode wavelet coefficient diagram of B_4^N .

3.2 Identification of damage severity

After the damage location of the beam structure is identified, the damage severity of the damage location is identified by PSO and IPSO, respectively. It can be determined whether the improvement of IPSO is effective through comparing the damage severity identification results of PSO and IPSO. The learning factor of PSO is set as $c_1 = c_2 = 2$, and other parameters are set the same as those of IPSO. Since the specific damage location of the right end of the beam cannot be identified, the damage severity of the nodes 48 and 50 of the right end of the beam are calculated.

According to Table 1 and Table 3, the fixed beams are modeled by MATLAB. The beam structure is equally divided into 49 elements according to the order of the beams from left to right in Figure 3. The left end point is taken as node 1 to the last element at the other end for node numbering in turn. The element stiffness is assembled according to the numbering order to obtain the overall stiffness, and then the modeling is completed. The PSO and IPSO running programs are compiled by MATLAB software, so that the damage severity can be calculated. Due to the randomness of intelligent algorithms in computation, PSO and IPSO run on the same computer ten times to reduce the randomness of their calculation, and the maximum and minimum will not be deleted from the results to ensure the fairness of each calculation result.

The severity graph and error graph of the structural damage identification by PSO are shown in Figure 7 and Figure 8, respectively.

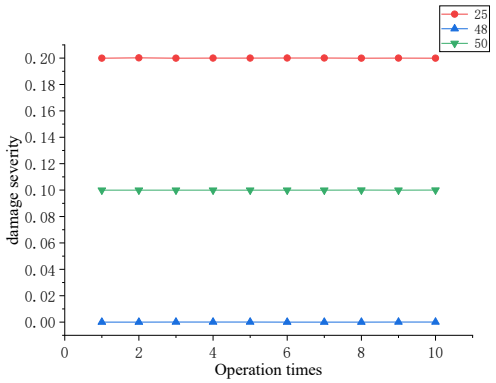

Figure 7: Damage severity identification of PSO

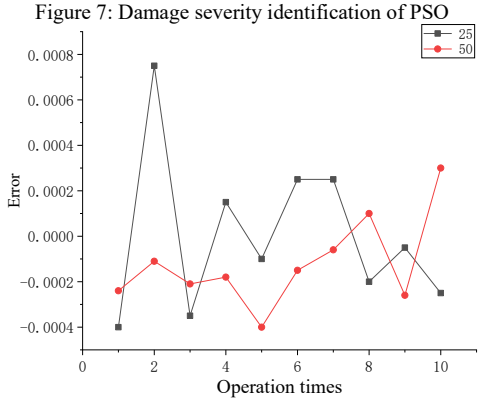

Figure 8: Error of PSO

International Journal of Innovative Research of Science, Engineering and Technology (IJIRSET)

Impact Factor 8.699

|www.ijirset.com |A Monthly, Peer Reviewed & Refereed Journal| e-ISSN: 2319-8753| p-ISSN: 2347-6710|

Volume 14, Issue 12, December 2025

|DOI: 10.15680/IJIRSET.2025.1412008|

Figure 7 and Figure 8 show that the error of PSO in identifying structural damage severity is within 0.8%, and the higher damage severity, the smaller fluctuation of damage error. In addition, the calculated result of node 50 has damage severity, while node 48 has no damage, it is indicated that the damage to the right end of the beam is element 49.

The severity graph and error graph of structural damage identification by IPSO are shown in Figure 9 and Figure 10, respectively.

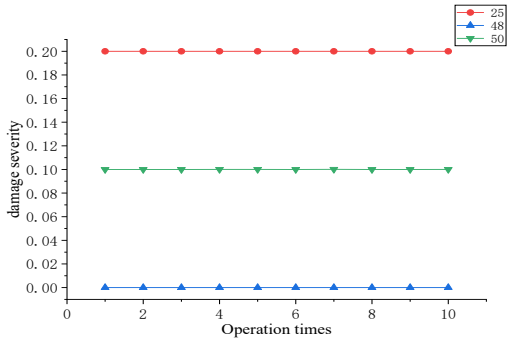

Figure 9: Damage severity identification of IPSO

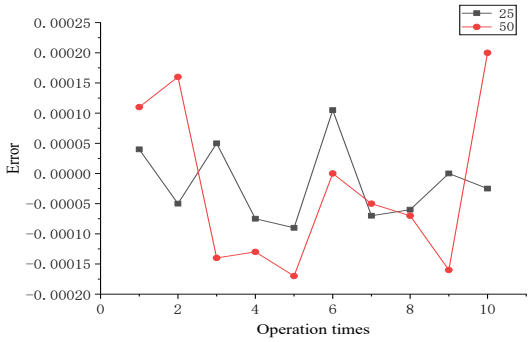

Figure 10: Error of IPSO

As shown in Figures 9 and 10, there is a higher accuracy in identifying the structural damage severity of IPSO than that of PSO, and its error is less than 0.2%, and the higher damage severity, the smaller damage error. In addition, the calculated result of node 50 has damage severity, while node 48 has no damage, it is indicated that the damage to the right end of the beam is element 49.

Table 4 shows the number of iterations and the time of ten calculations for PSO and IPSO. It can be found that the running time of IPSO is slightly longer than that of PSO, but the number of iterations is less than that of PSO, which indicates that the quality of each iteration of IPSO is higher than that of PSO.

Table 4: Iteration and objective function values of 0.8PSO and IPSO

Times	PSO		IPSO	
	Iterations	Time (s)	Iterations	Time (s)
1	68	476	62	496
2	68	473	60	486
3	69	486	59	489
4	69	479	62	501
5	67	480	64	506
6	69	482	61	492
7	68	477	61	504
8	69	472	62	499
9	70	483	60	497
10	68	481	63	493
Average value	68.5	478.9	61.4	496.3

International Journal of Innovative Research of Science, Engineering and Technology (IJIRSET)

Impact Factor 8.699

|www.ijirset.com |A Monthly, Peer Reviewed & Refereed Journal| e-ISSN: 2319-8753| p-ISSN: 2347-6710|

Volume 14, Issue 12, December 2025

|DOI: 10.15680/IJIRSET.2025.1412008|

In summary, the improvement of IPSO on the calculation method of learning factors is effective. IPSO can accurately identify the damage severity of the damage location and can also accurately locate the damage location.

IV. EXPERIMENT ANALYSIS

To verify the effectiveness of the proposed method in practice, a damage identification experiment is carried out on a fixed beam. Figure 11 shows the experiment, damage shape setting and grid setting of the beam elements, respectively. The parameters of the rectangular steel beam: Length $L=1300mm$, section size $b\times h=60mm\times 80mm$, other parameters are shown in Table 1. The damage scenario is shown in Table 3. The beam is evenly divided into 49 elements along the length direction, and $13mm$ is left at each end of the beam as the installation space of the vibration sensor. According to Figure 11 (c), the vibration sensor is installed on the grid node of the beam. The first column of data of the side near the upper surface along the length direction is the data of the first layer of the side, and then the data of the second, third and fourth layers of the side are successively approached to the lower surface of the beam. The beam is excited by percussion with a hammer, and the striking position is $20mm$-$40mm$ near the beam end. Sixteen high-sensitivity vibration sensors are installed on the grid nodes to collect modal data. After each batch of nodes is measured, the sensors are moved to the next batch of unmeasured nodes until the element nodes on the upper surface and side of the beam in Figure 11 (c) have measured. The data collected are processed by the DH5922D analysis system. Table 3 shows the damage scenario. The beam structural damage is manufactured by a milling machine with an accuracy of 0.1mm. The minimum size of the vibration sensor is $26mm$, so the minimum damage element size of the beam structure is set to $26mm$ to ensure that the node data information measured by the vibration sensor does not overlap.

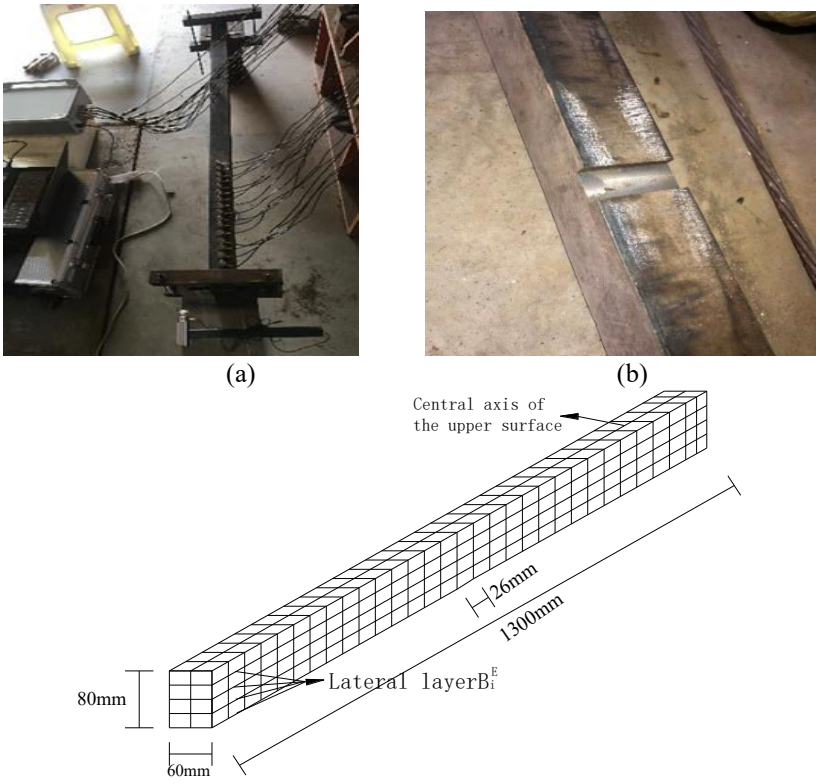

Figure 11: General situation of the experiment: (a) Sensor layout. (b) Damage setting. (c) Grid division of the beam.

4.1 Identification of damage location

According to the numerical simulation analysis, only five sets of data are needed for the experiment beam to identify the damage. The sensor can not measure the strain mode directly, but can measure the displacement mode, so the five groups of experiment data are displacement mode data. Then, the strain mode is obtained by second-order difference of

International Journal of Innovative Research of Science, Engineering and Technology (IJIRSET)

Impact Factor 8.699

|www.ijirset.com |A Monthly, Peer Reviewed & Refereed Journal| e-ISSN: 2319-8753| p-ISSN: 2347-6710|

Volume 14, Issue 12, December 2025

|DOI: 10.15680/IJIRSET.2025.1412008|

the five groups of displacement modal data, respectively, and the modal data are denoised by the wavelet toolbox of MATLAB. The normalization formula of strain modal data is shown in equation (19).

DB3 wavelet is used to transform the strain modes, and the wavelet coefficients of the strain mode of the central axis on the upper surface and the side of the beam are obtained, respectively, as shown in Figure.12. Nodes 10, 11, 22, 23, 24, 46, 47 and 48 in Figure 12 (a) show singularity. According to the position of the maximum modulus of the wavelet coefficient are nodes 10 and 23, which correspond to the damage position of elements 12 and 25, it can be preliminarily determined that the damage of the beam along the length direction are elements 12 and 25. Due to the edge effect of the wavelet coefficient and the limitation of the data length of the right end, it is difficult to determine the specific damage location of the right end of the beam. Figure 12 (b) ~ (e) show that as the wavelet coefficient diagram gets closer and closer to the fourth layer of the beam (that is, the bottom surface of the beam), the modulus maximum of the wavelet coefficient at node 23 keeps increasing, and the absolute value of the wavelet coefficient singularity at the fourth layer of the beam is the largest. Node 23 corresponds to element 25, so it can be determined that the damage location of element 25 along the height direction is located on the bottom surface of the beam. The wavelet coefficients of element 12 in Figure 12 (b) ~ (e) do not show an obvious singularity, which indicates that the damage of element 12 along the beam height direction is not identified. By comparing the wavelet coefficients around element 49 in Figure 12 (b) ~ (e), it can be found that there are no singular points around element 49 except for element 49, which indicates that there is no damage around element 49, while Figure 12 (a) indicates that there is damage around element 49, so element 49 can be determined as the damaged element. Due to the inevitable errors in the experiment, and the third and fourth layers on the side of the beam are adjacent data layers, there is an error in determining the damage coordinates of element 49 in the height direction, but it can be roughly concluded that the damage is located at the third and fourth layers in the height direction.

In conclusion, it can be concluded that there are three spatial damages in the beam structure, which are: element 12 in the length direction, with unknown height; element 25 in the length direction, with a height of the fourth floor (that is, the bottom of the beam); element 49 in the length direction, with heights of the third and fourth floors. The beam structural experiment shows that the damage method based on 3D-slicing can effectively identify the spatial damage location. Through the analysis of Figure 12, it can be seen that in the case of insufficient data, the damage location of the beam structure can be preliminarily identified by comparing the absolute value of the wavelet coefficient singularity. In the actual damage identification of the beam structure, the proposed method can initially identify small damage with a severity of 5%, but cannot completely identify the overall spatial location, which is different from the conclusion of numerical simulation, indicating that the proposed method has a better damage identification effect in practice. In the same scenario, the absolute value of the wavelet coefficient singularity corresponding to the damage location and the range of wavelet coefficient singular increase with the increase of the damage severity, which is consistent with the conclusion of the numerical simulation.

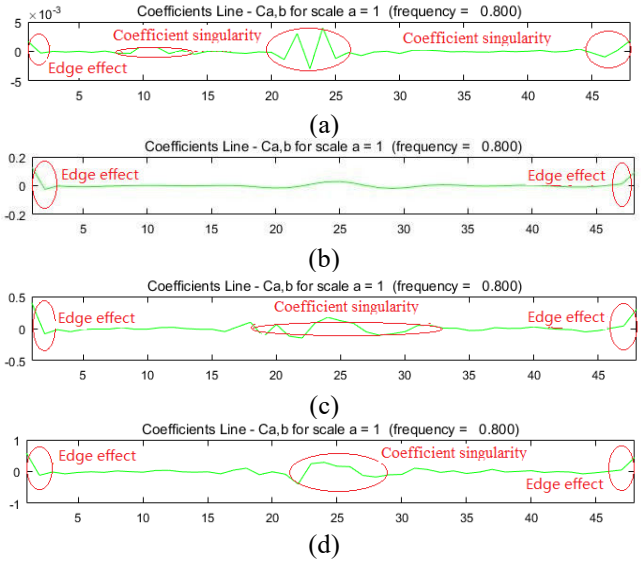

International Journal of Innovative Research of Science, Engineering and Technology (IJIRSET)

Impact Factor 8.699

|www.ijirset.com |A Monthly, Peer Reviewed & Refereed Journal| e-ISSN: 2319-8753| p-ISSN: 2347-6710|

Volume 14, Issue 12, December 2025

|DOI: 10.15680/IJIRSET.2025.1412008|

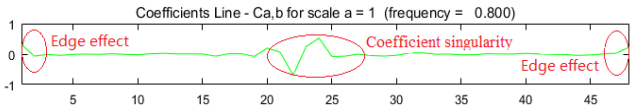

(e)

Figure 12: Wavelet coefficients of strain modes of the beam structural upper surface and lateral surface.(a) The strain mode wavelet coefficients of the central axis of the beam structural upper surface. (b) The strain mode wavelet coefficient diagram of B_1^E. (c) The strain mode wavelet coefficient diagram of B_2^E. (d) The strain mode wavelet coefficient diagram of B_3^E. (e) The strain mode wavelet coefficient diagram of B_4^E.

4.2 Identification of damage severity

After the damage location of the beam structure is identified, the damage severity of the damage location is identified by PSO and IPSO, respectively. It can be determined whether the improvement of IPSO is effective through comparing the damage severity identification results of PSO and IPSO. The learning factor of PSO is set as $c_1 = c_2 = 2$, and other parameters are set the same with IPSO.

According to Table 1 and Table 3, the fixed beams are modeled by MATLAB. The beam structure is equally divided into 49 elements according to the order of the beams from left to right in Figure 3. The left end point is taken as node 1 to the last element at the other end for node numbering in turn. The element stiffness is assembled according to the numbering order to obtain the overall stiffness, and then the modeling is completed. The PSO and IPSO running programs are compiled by MATLAB software, so that the damage severity can be calculated. Due to the randomness of intelligent algorithms in computation, PSO and IPSO run on the same computer ten times to reduce the randomness of calculation, and the maximum and minimum will not be deleted from the results to ensure the fairness of each calculation result.

The experiment data are affected by human factors, specimen manufacturing errors and noise, so it is necessary to denoise the experiment data through a denoising tool in MATLAB wavelet toolbox, and then the damage severity is identified. The minimum absolute error of IPSO for identifying the severity of damage at three locations is 1.342%, while the minimum absolute error of PSO is 1.551%. According to the identification results, the error of damage height recognition is calculated. The damage stiffness calculation formula is shown in equation (20), h_i is the height of the damage element. The calculation results of IPSO are shown in Table 5.

$$I = \frac{1}{12} b h_i^3 \qquad (20)$$

Table 5: Calculation results of h_i

	γ =5%		γ =20%		γ =10%	
	h_i(mm)	(h-h_i)/h (%)	h_i(mm)	(h-h_i)/h (%)	h_i(mm)	(h-h_i)/h (%)
1	78.2826	2.1468	72.9202	8.8497	76.5540	4.3076
2	78.2561	2.1798	72.9228	8.8465	76.5566	4.3043
3	78.2790	2.1513	72.9218	8.8477	76.5604	4.2995
4	78.2701	2.1624	72.9205	8.8493	76.5752	4.2810
5	78.2595	2.1757	72.9208	8.8489	76.5554	4.3057
6	78.2634	2.1708	72.9379	8.8277	76.5738	4.2828
7	78.2762	2.1548	72.9314	8.8357	76.5720	4.2850
8	78.2776	2.1530	72.9106	8.8618	76.5583	4.3021
9	78.2776	2.1530	72.9225	8.8469	76.5706	4.2868
10	78.2745	2.1569	72.9208	8.8489	76.5708	4.2864

In summary, the improvement of IPSO on the calculation method of learning factors is effective. IPSO can accurately identify the damage severity of the damage location and can also accurately identify the damage location.

V. CONCLUSION

Aiming at the problem of the spatial damage identification of the beam structure, a method based on 3D-slicing is proposed. The beam structure is sliced according to three-dimensional direction to achieve the purpose of dimensionality reduction and simplification of the damage recognition principle. The damage coordinates of the

International Journal of Innovative Research of Science, Engineering and Technology (IJIRSET)

Impact Factor 8.699

|www.ijirset.com |A Monthly, Peer Reviewed & Refereed Journal| e-ISSN: 2319-8753| p-ISSN: 2347-6710|

Volume 14, Issue 12, December 2025

|DOI: 10.15680/IJIRSET.2025.1412008|

beam structure in each dimensional direction are identified by wavelet transform, to realize the spatial damage location recognition of the beam structure. The conclusions are as follows:

(1) IPSO is proposed to improve the calculation method of learning factors in PSO, which solves the problem that PSO is prone to fall into prematurity and local optimal solution in this study. By comparing the results of POS and IPSO in numerical simulation and experimental analysis of the beam structure, it is proved that the improvement of IPSO is effective, and IPSO can accurately identify the damage severity of the beam structure, and can accurately identify the suspected damage location.

(2) In this study, it is concluded that the greater the severity of damage of the same structure under the same scenario, the greater the absolute value of the singularity of wavelet coefficients and the singularity range of wavelet coefficients. This conclusion helps to identify the spatial damage of the beam structure, but also provides a solution to the problem that edge damage is difficult to identify due to the edge effect of the wavelet coefficient.

(3) Through the numerical simulation and experimental analysis of the beam structure, it is proved that the spatial damage of the beam structure can be accurately identified through the 3D-slicing method based on strain modal parameters, and the problem that it is difficult to identify the spatial damage of the structure based on wavelet transform and intelligent algorithm is solved by 3D-slicing method. This method provides technical support for the spatial damage identification of actual beam structures, and can also be used as a reference method for other structures.

The proposed method opens up a new way for spatial damage identification of the beam structure, which can provide a theoretical basis and technical support for the actual damage identification of the beam structure. However, the proposed method has poor effective in the identification of minor damage, so it is necessary to improve the identification accuracy of minor damage and study the effectiveness of the method in damage identification of other structures in the future.

V. ACKNOWLEDGMENTS

The authors gratefully acknowledge financially supported by the National College Student Innovation and Entrepreneurship Training Program Project (no. S202311527027). The supports are gratefully acknowledged.

REFERENCES

[1] X. J. Liu, L.J. Xiang, and S. X. Zhang, “Simply supported beam bridge damage identification based on wavelet transform,” *Journal of Vibration, Measurement & Diagnosis,* vol. 35, no. 5, pp. 866-872+990, 2015.（in Chinese）

[2] M. Abdulkareem, N. Bakhary, and M. Vafaei , et al., “Application of two-dimensional wavelet transform to detect damage in steel plate structures,” *Measurement*, vol. 146, pp. 912–923, 2019.

[3] Y. C. REN, J. F. Zhang, and Z. F. Liu, et al., “The method for damage identification of reinforced concrete beams based on wavelet packet,” *Journal of Vibration, Measurement & Diagnosis*, vol. 31, no. 5, pp. 605-609+665, 2011.（in Chinese）

[4] W. Fan, and P. Qiao, “Vibration-based damage identification methods: a review and comparative study,” *Struct Health Monit*, vol. 10, no. 1, pp. 83–111, 2011.

[5] C. Zhang, L. Cheng, and J. Qiu, et al., “Structural damage detections based on a general vibration model identification approach,” *Mechanical Systems and Signal Processing*, vol. 123, pp. 316-332, 2019.

[6] H. Lopes, J.V. Araújo dos Santos, and A. Katunin, “Identification of material properties of a laminated plate from measurements of natural frequencies and modal rotations,” *Procedia Structural Integrity*, vol. 17, pp. 971-978, 2019.

[7] E. P. Carden, and F. N. P, “Vibration based condition monitoring: a review,” *Struct Health Monit*, vol. 3, no. 4, pp. 355–377, 2004.

[8] Y. Yan, L. Cheng, and Z Wu, et al., “Development in vibration-based structural damage detection technique,” *Mech Syst Signal Process*, vol. 21, no. 5, pp. 2198–2211, 2007.

[9] Z. Y. Shi, S. S. Law, and L. M. Zhang, “Structural damage localization from modal strain energy change,”,*Journal of Sound and Vibration*, vol. 218, no. 5, pp. 825-844,1998.

International Journal of Innovative Research of Science, Engineering and Technology (IJIRSET)

Impact Factor 8.699

|www.ijirset.com |A Monthly, Peer Reviewed & Refereed Journal| e-ISSN: 2319-8753| p-ISSN: 2347-6710|

Volume 14, Issue 12, December 2025

|DOI: 10.15680/IJIRSET.2025.1412008|

[10] D. Q. Guan, and Y. Huang, "Damage identification of elastic foundation beams based on wavelet transform of rotation angle modes," *Journal of vibration and shock*, vol. 27, no. 5, pp. 44-47,2008.（in Chinese）
[11] L. Y. Yam, T. P. Leung, and D. B. Li, et al., "Theoretical and experimental study of modal strain analysis, *Journal of Sound & Vibration*," vol. 191, no. 2, pp. 251-260,1996.
[12] Z. D. Xu, and K. Y. Xu, "Damage detection for space truss structures based on strain mode under ambient excitation," *Journal of Engineering Mechanics*, vol. 138, no. 10, pp. 1215-1223, 2012.
[13] S. Wu, J. Zhou, and S. Rui, et al., "Reformulation of elemental modal strain energy method based on strain modes for structural damage detection," *Advances in Structural Engineering*, vol. 20, no. 6, pp. 896-905, 2016.
[14] I. M. D. Rosa, C. Santulli, and F. Sarasini, "Acoustic emission for monitoring the mechanical behaviour of natural fibre composites: a literature review," *Composites part a: applied science and manufacturing*, vol. 40, pp. 1456–1469, 2009.
[15] M. Abdulkareem, N. Bakhary, and M. Vafaei, et al., "Experimental damage assessment of support condition for plate structures using wavelet transform," *Journal of Theoretical and Applied Mechanics*, vol. 57, no. 2, pp. 501-518, 2019.
[16] X. Q. Zhu, and S. S. Law, "Wavelet-based crack identification of bridge beam from operational deflection time history", *International Journal of Solids and Structures*, vol. 43, no. 7, pp. 2299–2317, 2006.
[17] W. Y. He, S. Y. Zhu, and W. X. Ren, "Two-phase damage detection of beam structures under moving load using multi-scale wavelet signal processing and wavelet finite element model," *Applied Mathematical Modelling*, vol. 66, pp. 728-744, 2019.
[18] J. Zhou, and L. Zheng, "Damage detection based on vibration for composite sandwich panels with truss core," *Composite Structures*, vol. 229, pp. 111376, 2019.
[19] L. Nguyen-Ngoc, N. H. Tran, and T. Bui-Tien, et al., "Damage detection in structures using particle swarm optimization combined with artificial neural network," *Smart Structures and Systems*, vol. 28, no. 1, pp. 1–12, 2021.
[20] F. Jiang, H. Xia, and Q. A. Tran, et al., "A new binary hybrid particle swarm optimization with wavelet mutation, Knowledge-Based Systems," *Knowledge-Based Systems*, vol. 130, no. 15, pp. 90-101, 2017.
[21] C. L. T, N. N. T, and K. S, et al., "An efficient approach for damage identification based on improved machine learning using PSO-SVM," *Engineering with Computers*, pp.1-16, 2021.
[22] A. T. F, K. S, and B. B, et al., "A hybrid PSO and Grey Wolf Optimization algorithm for static and dynamic crack identification," *Theoretical and applied fracture mechanics*, vol. 118, pp. 103213, 2022.
[23] H. L. Minh, S. Khatir, and R. V. Rao, et al., "A variable velocity strategy particle swarm optimization algorithm (VVS-PSO) for damage assessment in structures," *Engineering with Computers*, pp.1-30, 2021.
[24] S. Khatir, T. Khatir, and D. Boutchicha, et al., "An efficient hybrid TLBO-PSO-ANN for fast damage identification in steel beam structures using IGA," *Smart Structures and Systems*, vol. 25, no. 5, pp. 605-617, 2020.
[25] D. Gogolewski, "Influence of the edge effect on the wavelet analysis process," *Measurement*, vol.152, pp. 107314, 2020.
[26] M. Y. WANG, B. R. MIAO, and X. J. LI, et al., "Damage Identification of Continuous Beam Based on Rotation Mode and Wavelet Neural Network," *Chinese Quarterly of Mechanics*, vol. 37, no. 4, pp. 684-691, 2016.（in Chinese）
[27] F. LI，G. MENG, and K. Kageyama, et al, "Optimal Mother Wavelet Selection for Lamb Wave Analyses," *Journal of Intelligent Material Systems & Structures*，vol. 20, no. 10, pp. 1147-1161, 2009.
[28] TAHA, and M. M. R, "Wavelet Transform for Structural Health Monitoring: A Compendium of Uses and Features," *Structural Health Monitoring*，vol. 5, no. 3, pp. 267-295, 2006.
[29] J. Guo, D. Q. Guan, and J. W. Zhao, "Structural damage identification based on the wavelet transform and improved particle swarm optimization algorithm," *Advances in Civil Engineering*, vol. 2020, pp. 1-19, 2020.
[30] M. Hanteh, and O. Rezaifar, "Damage detection in precast full panel building by continuous wavelet analysis analytical method," *Structures*, vol. 29, pp. 701-713, 2021.

INTERNATIONAL STANDARD SERIAL NUMBER INDIA

INNO SPACE SJIF Scientific Journal Impact Factor

doi cross ref

निस्केयर NISCAIR

INTERNATIONAL JOURNAL OF INNOVATIVE RESEARCH

IN SCIENCE | ENGINEERING | TECHNOLOGY

9940 572 462 6381 907 438 ijirset@gmail.com

www.ijirset.com

Scan to save the contact details